

# Globular Cluster formation in a collapsing supershell

S. Recchi<sup>1</sup> • R. Wünsch<sup>1</sup> • J. Palouš<sup>1</sup> •  
F. Dinnbier<sup>1</sup>

**Abstract** Primordial clouds are supposed to host the so-called population III stars. These stars are very massive and completely metal-free. The final stage of the life of population III stars with masses between 130 and 260 solar masses is a very energetic hypernova explosion. A hypernova drives a shock, behind which a spherically symmetric very dense supershell forms, which might become gravitationally unstable, fragment, and form stars. In this paper we study under what conditions can an expanding supershell become gravitationally unstable and how the feedback of these supershell stars (SSSs) affects its surroundings. We simulate, by means of a 1-D Eulerian hydrocode, the early evolution of the primordial cloud after the hypernova explosion, the formation of SSSs, and the following evolution, once the SSSs start to release energy and heavy elements into the interstellar medium. Our results indicate that a shell, enriched with nucleosynthetic products from SSSs, propagates inwards, towards the center of the primordial cloud. In a time span of a few Myr, this inward-propagating shell reaches a distance of only a few parsec away from the center of the primordial cloud. Its density is extremely high and its temperature very low, thus the conditions for a new episode of star formation are achieved. We study what fraction of these two distinct populations of stars can remain bound and survive until the present day. We study also under what conditions can this process repeat and form multiple stellar populations. We extensively discuss whether the proposed scenario can help to explain some open questions of the formation mechanism of globular clusters.

**Keywords** dark ages, reionization, first stars; ISM: supernova remnants; stars: formation; globular clusters: general

## 1 Introduction

The evolution of a spherically symmetric blast wave expanding into the interstellar medium (ISM) is a well-established, textbook topic, amply covered in many highly detailed reviews (see e.g. Ostriker & McKee 1988; Bisnovatyi-Kogan & Silich 1995). After the relatively short free expansion and adiabatic phases, the gas just behind the outward-propagating shock cools and forms a very dense shell of material which continues propagating outwards due to its inertia.

The stability of this thin shell of gas has been also extensively studied (e.g. Vishniac 1983; Whitworth et al. 1994a,b; Elmegreen 1994; Ehlerova et al. 1997; Wünsch & Palouš 2001; Dinnbier et al. 2017, see also Sect. 2). Unstable modes can be found for a wide range of initial conditions, and the fragmentation of the unstable supershell can lead to star formation. This has been proposed as a possible triggering mechanism for star formation (e.g. Gerola & Seiden 1978; Elmegreen & Elmegreen 1978; Palous et al. 1994). Stars formed in this still outward-propagating supershell will evolve and release winds and, possibly, supernova (SN) explosion, into the ISM like any other stellar system. However, the evolution of the supershell and of the stellar ejecta after the formation of the supershell stars (SSSs) is still largely unexplored. Our intention is to fill this gap.

Gravitationally unstable supershells may also be related to the formation of globular clusters (GCs). In particular, the lack of GCs with a metallicity below  $[\text{Fe}/\text{H}] \simeq -2.5$  (Harris 1996) has puzzled astronomers for a long time. It seems possible to explain this fact

---

S. Recchi  
R. Wünsch  
J. Palouš  
F. Dinnbier

Astronomical Institute, Academy of Sciences of the Czech Republic, Boční II 1401-2a, Prague, Czech Republic  
Email: simone.recchi@asu.cas.cz

by assuming an early generation of stars at the center of a proto-GC. Supernovae go off and create an expanding supershell. The mixing of the expanding supershell with the ejecta of the first generation of stars lead to the right metal enrichment (Brown et al. 1991; Parmentier et al. 1999; Recchi & Danziger 2005; Shustov & Wiebe 2000). In particular, if the mass of the proto-GC is larger than some threshold (usually in the range of  $10^6$ - $10^7$   $M_\odot$ ), the fragmentation of the supershell can occur before the supershell becomes gravitationally unbound. This guarantees that the newly-formed SSSs will remain bound to the cluster.

However, it is unlikely that this scenario can explain all chemical properties of GCs. These properties are reviewed in Sect. 2, but in brief GCs are characterized by multiple stellar populations and by characteristic anti-correlations between some pairs of light elements. Particularly remarkable and ubiquitous are the Na-O and Mg-Al anticorrelations (see e.g. Sneden et al. 1997; Gratton et al. 2004, and references therein,) notice however that the Mg-Al anticorrelation is ubiquitous only in massive GCs and often is missing in less massive ones (see e.g. Pancino et al. 2017, and references therein). On the other hand, there is a remarkable homogeneity in the abundances of iron-peak elements in the large majority of observed GCs. The scenario depicted above seems thus unlikely because it implies that the stars which created and enriched the expanding supershell in iron either disappeared or had already the relatively high  $[\text{Fe}/\text{H}]$  we observe nowadays. Other scenarios have therefore been proposed to explain the peculiar chemical properties of GCs. These scenarios are very briefly reviewed in Sect. 2.

However, it is maybe possible to save the broad scenario (fragmentation in the expanding supershell) by invoking a different trigger for the supershell expansion, namely a primordial, very energetic population-III (Pop-III) star. This can also easily explain the relatively high iron content of observed GCs (Beasley et al. 2003). The stars formed in this expanding supershell will evolve as any normal star: they will create stellar winds and, depending on the IMF, some of them will explode as Type II supernovae (SNeII). Some of the winds of these SSSs will propagate inwards rather than outwards. They might accumulate in the center (or close to the center) of the proto-GC, cool and condense there, maybe leading to a new episode of star formation. This is the general idea we want to explore here and in follow-up papers. The paper is structured as follows: in Sect. 2 we will briefly summarize the main physical and chemical properties of GCs and what features a theory of GC formation must have in order to reproduce them. We will then lay down the idea of the paper

in more detail in Sect. 3.1, linking the proposed model to the requisites of theories of GC formation described in Sect. 2. The initial conditions are presented in Sect. 3.2, the adopted numerical scheme in Sect. 3.3, the assumed criteria for the fragmentation of the expanding supershell in Sect. 3.4, and the results of numerical experiments in Sect. 4. Specifically, in Sect. 4.1 we study the expanding supershell and the formation of the 1G SSSs, in Sect. 4.2 we study the fate of the inward-propagating supershell formed by the SSSs winds, and we establish under what conditions this supershell can form a new generation of stars and what are the characteristics of these second-generation stars. Finally, in Sect. 5 we will discuss our results and draw conclusions.

## 2 The properties of globular clusters

GCs show characteristics which have puzzled astronomers for decades. Many theories of their formation have been put forward but none of them manage to explain all properties of GCs. This lead Bastian (2015) to write "Hence, with the exclusion of all current models, new scenarios are desperately needed." Many review papers describe in detail the chemical characteristics of GCs and the properties a theory of GC formation should have in order to conform with observations (see in particular Bastian 2015; Renzini et al. 2015). We will follow in particular Renzini et al. (2015), grossly simplifying the description. We refer to the original paper for more detail.

1. **Specificity.** A crucial property of GCs is the presence of multiple populations of stars, with a number of different stellar populations ranging from two to perhaps seven (Milone et al. 2015a). This phenomenon appears to be specific of GCs: young massive clusters do not show clear evidence of multiple populations although the masses of these clusters are similar (see recent papers by Bastian et al. 2013a; Cabrera-Ziri et al. 2016). It seems thus, to quote Renzini et al. (2015), that "special conditions encountered only in the early Universe appear to be instrumental for the occurrence of the GC multiple population phenomenon." *We identify in this work these "special conditions" with the explosion of very massive pop-III stars*, as we describe in detail in Sect. 3.1. Another aspect of the specificity of GCs is the fact that field halo stars with the same metallicity and age do not show the same chemical characteristics of GC stars. On the other hand, we note that Niederhof et al. (2017) recently reported the discovery of multiple stellar populations in 3 intermediate-age star clusters in the Small Magellanic Cloud.

2. **Predominance.** At least half of the stars in GCs have been self-polluted within the GC, thus do not belong to the first generation (1G) of stars. This is strictly connected to the so-called mass-budget problem: a significant mass in ejecta from 1G pollutant stars is required to explain the fraction of late-generation (LG) stars but, for ordinary IMFs, 1G ejecta constitute only a small fraction of the total 1G mass. The fraction of 1G stars could be as low as one third and pretty constant among different GCs (Bastian & Lardo 2015), although a more recent study shows a clear variability of this fraction and an anti-correlation with the GC mass (Milone et al. 2017). In particular, the smallest GCs show 1G fractions larger than 50%, whereas this fraction decreases to about 20% for the most massive GCs. Notice that the mass dependence is not limited to the 1G stellar fraction. Also the spread in helium (Milone 2015) and in light elements (Milone et al. 2017) seems to correlate with the GC mass.
3. **Discreteness.** The process of star formation in GCs appears to be discontinuous, characterized by well-separated events. This is clearly visible in well-separated main sequences in color-magnitude diagrams (Piotto et al. 2007). This is much less clear in the apparently continuous Na-O and Mg-Al anticorrelations, although at least in the Na/O plane discrete multiple populations are discernible (Marino et al. 2008; Milone et al. 2015b) and signs of patchiness in the distribution of other chemical elements have started to emerge (Carretta 2015).
4. **Supernova avoidance.** As already mentioned, stars in the large majority of GCs do not show a spread in iron-peak or in other heavy elements, clearly showing that SN ejecta should negligibly contribute to the chemical enrichment of LG stars. However, it is worth mentioning that the fraction of observed GCs which shows also a spread in heavy elements is increasing by the day and nowadays amounts to about 15 to 20% of the observed GCs (see in particular Marino et al. 2015, and references therein). This variation is not limited to iron-peak elements but it is extended to calcium and s-process elements. This has been shown in a number of objects (see e.g. Marino et al. 2011; Johnson et al. 2017; Milone et al. 2015a; Yong et al. 2014, 2016). SNe might therefore play after all a role in the evolution of some GCs.

There are other peculiar characteristics of GC stars and constraints for theories of GC formation. In particular, a theory of GC formation should be able to reproduce the above mentioned Na-O and Mg-Al anticorrelations, and should reproduce the observed spread

in He. We will not treat these aspects in detail, as they are more closely related to the nucleosynthesis of stars within a GC rather than to the mechanism of GC formation.

As already mentioned, various models have attempted to explain the peculiarities of GC stars. We refer again to review papers for a detailed description. We recall here very briefly only the two more widely investigated scenarios:

- **Pollution from winds of massive stars, e.g. from fast rotating massive stars (FRMS)** (Charbonnel & Chantreau 2016; Krause et al. 2013; Decressin et al. 2007; Wünsch et al. 2016, 2017; Lochhaas & Thompson 2017). The idea is that extruding disks of FRMS, filled with ejecta from stellar winds, mix with pristine gas and form new generations of stars.
- **Pollution from AGB stars** (D’Ercole et al. 2008, 2010) Here the assumption is that the ejecta of AGB stars, given their low velocity, might remain bound to the proto-GC, whereas SN remnants do not. The AGB ejecta, possibly mixed with some pristine material, form LG stars.

Both these scenarios, and many other scenarios not described here (see e.g. de Mink et al. 2009; Bastian et al. 2013b; Denissenkov et al. 2015) have attractive features, as well as some problems which require some tweaking of parameters.

### 3 The proposed model

#### 3.1 General idea

We recall here the main aim of our paper. We want to study the fragmentation of a supershell created by the explosion of a Pop-III star and the fate of winds of stars formed out of this fragmented supershell. It is to be expected that approximately a half of these winds will propagate towards the center of the system (the place where the Pop-III star exploded), perhaps creating the conditions for a new episode of star formation. In fact, the density of gas piling up close to the center must increase, thus the cooling increases too, leading to large regions of cold, dense gas, probably prone to the formation of new stars. Alternatively, the inward-propagating winds of SSSs could trigger the formation of another inward propagating dense supershell, able to fragment itself and form a new generation of stars. At the same time, the SSSs destroy by their winds the primary expanding shell and a fraction of them leaves the proto-cluster due to their outward velocity inherited from the expanding shell, in combination with galactic

tides. This process might then repeat itself. We illustrate the main phases of our assumed scenario in Fig. 1.

We believe that this study is interesting per se, as we are not aware of similar studies in the literature, but we want to explore here the possibility that this mechanism is connected to the formation of GCs. We will thus go through the points illustrated in Sect. 2 (specificity, predominance, discreteness, SN avoidance) and analyze if our proposed scenario might help explaining them. Ours is thus not properly a scenario of progenitors of polluted GC stars (as the massive stars and the AGB scenarios are). We think that many authors (many of them mentioned above) have made a great job trying to identify the nucleosynthesis pathways towards the chemical patterns observed in GCs. We simply devise a possible evolutionary pathway which might help solve some of the difficulties encountered by these progenitor models. For convenience we tune our discussion and the following calculations to the massive stars scenario, but we believe that with simple changes our idea can be adapted to the AGB scenario (and perhaps to the other proposed scenarios) as well.

1. **Specificity.** This is easy: stars in GCs appear unlike stars in young massive clusters because nowadays Pop-III stars do not exist any more, thus our proposal can apply preferentially to very old massive clusters, not to young ones. Our scenario requires a very energetic Pop-III star, able to sweep up a large mass of gas. The properties and nucleosynthesis of these extremely massive ( $M > 100 M_{\odot}$ ) stars are pretty well known (e.g. Heger & Woosley 2002). Attention in the last few years has shifted to less massive ( $M < 100 M_{\odot}$ ) first stars (e.g. Heger & Woosley 2010; Choplin et al. 2016). This is most probably due to the need to explain the observed chemical composition of ultra metal-poor stars (e.g. Placco et al. 2016), which are extremely poor in iron, thus can not have been polluted by very massive Pop-III stars. It is nevertheless still true that, due to the lack of metals and to the higher temperature of the cosmic microwave background, the conditions in the early universe should have favoured the formation of very massive stars (Bromm et al. 1999). Therefore it appears to us plausible that very massive Pop-III stars existed in the early universe, and were responsible for the formation of GCs. The high iron yields of these Pop-III stars are responsible for the relatively high  $[\text{Fe}/\text{H}]$  in observed GCs (Beasley et al. 2003). Less massive (and less energetic) Pop-III stars were, on the other hand, unable to sweep up large masses of pristine gas and were thus unable to trigger the formation of large clusters. They polluted the ISM more patchily, creating

the conditions for the formation of ultra metal-poor stars. Recently, Elmegreen (2017) suggested that the different conditions that allowed the formation of GCs in the early universe were due to the higher densities. This is of course a viable suggestion, alternative to our proposed Pop-III triggered mechanism.

2. **Predominance.** The problem of the predominance (and the associated problem of the mass budget) is typically solved assuming that the 1G stars we see nowadays in a GC are just a small fraction of the polluting stars originally present in the proto-cluster. However, no convincing scenario has been put forward to explain why a large fraction of 1G stars should leave the proto-GC. Our proposed scenario might provide a partial solution because (i) the SSSs possess a positive radial velocity (they inherit the velocity of the supershell). Some of the SSSs might have a velocity larger than the escape velocity from the proto-GCs. On the other hand, the winds from these SSSs will have at least partially a negative radial velocity, assuming that they expand isotropically from the SSSs and that their velocities are larger than the stellar velocities. (ii) Even if SSSs do not escape directly, they are formed at relatively large distances from the center of the cluster. As they start being pulled towards the cluster center, they will acquire relatively large velocities. The velocity dispersion of SSSs (the 1G stars in our scenario) will be thus larger than the velocity dispersion of stars formed closer to the center of the cluster, thus it is less likely that they will be bound to the cluster. At least in principle, our model can explain the anticorrelation between cluster mass and 1G star fraction (and between mass and chemical complexity) described in Sect. 2. According to our model, a crucial parameter is the fragmentation time of the supershell (see Sect. 3.4); for large fragmentation times, the supershell can propagate further and collect more mass. The larger mass in SSSs does not necessarily imply a larger mass in 1G stars. Having formed at large radii, a large fraction of the SSSs might be unbound and leave the proto-GC. On the other hand, the SSS ejecta are more massive and therefore a larger fraction of 1G stars can be formed. This can explain the anti-correlation between cluster mass and 1G star fraction. Moreover, as already mentioned (and as we will see below), a new generation of stars can be formed in an inward-propagating shell. The radius at which this shell will fragment and form new stars will depend on the radius at which SSSs form. If the fragmentation radius of the inward-propagating shell is large enough, this process can repeat itself (see also below).



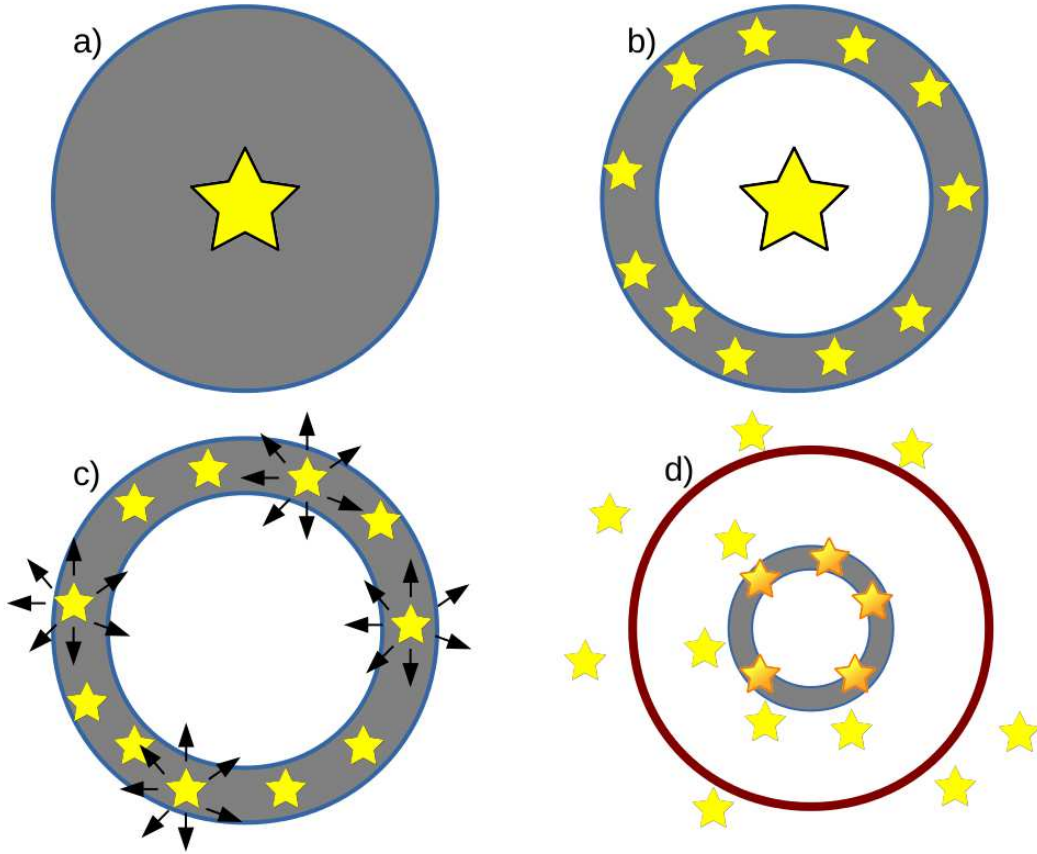


**Fig. 1** The major phases of our assumed scenario for the formation of GC: *a)* A very massive pop-III star explodes in the middle of a primordial cloud, *b)* The energy of this star produces a shell of dense, cold gas. This supershell becomes gravitationally unstable, fragments and forms new stars (1G stars) *c)* Supershell stars release energy, due to stellar winds and SN explosions. Some of the gas they release is driven inwards. *d)* This triggers the formation of a new, inward-propagating supershell, which fragments and forms a second generation of stars. The thick red line denotes the tidal radius in the external proto-galactic field.

3. **Discreteness.** It is obvious that 1G stars and LG stars are well-separated. 1G stars are the surviving SSSs, whereas LG stars are formed later, closer to the center of the cluster. To explain the presence of multiple ( $n > 2$ ) separated generations of stars, we must assume that the mechanism we describe here might replicate itself: SSSs form an inward-propagating shell, which fragments and form new stars, which create another inward-propagating supershell, and so on. As we will see in Sect. 4.2, simulations suggest that this mechanism might be possible. Moreover, as explained above, this mechanism might depend on the fragmentation time of the supershell (and thus on the radius at which SSSs form). This can affect the fragmentation radius of the inward-propagating shell, which in turn will affect the probability that this mechanism repeats itself. We see thus, at least in principle, a possible ex-

planation for the correlation between GC mass and chemical complexity (spread in helium and in light elements) described in Sect. 2. The larger the fragmentation time, the larger the collected supershell mass, the larger the mass in LG stars, the larger the probability of forming multiple (and not just two) stellar population, the larger the chemical complexity.

4. **Supernova avoidance.** In the framework of the massive stars, we must assume that the processes leading to the formation of LG stars should occur relatively quickly (within few Myr), in order to be completed before SNeII go off. As we will see below, again, simulations (and analytical considerations) seem to support this view. However, as remarked in Sect. 2, a non-negligible fraction of GCs do show a spread in heavy elements, which may be due to differences in their supplies by Pop-III stars of different

mass, or due to changing fragmentation time of the supershell. Some of these GCs (as originally suggested for the archetypal examples of Omega Centauri and M22) might be remnants of tidally disrupted dwarf galaxies (see e.g. Marino et al. 2015) but, for some others, an internal mechanism might be invoked. This is easily accounted for, if the formation of LG stars lasts more than a few Myr (see also Sect. 4.2).

After having laid down the general idea of this paper, we describe here and in the following section the calculations we have performed to substantiate it. The calculations presented here should be seen as a feasibility study rather than as a complete, self-consistent description of the phenomena we wish to simulate. A fully consistent simulation requires the inclusion of many complex physical processes and is very computationally demanding. Before embarking on this kind of computation, we want to be sure that the proposed scenario can really work, thus we will present here a simplified model. Even this simplified model turns out to be more computationally demanding than we thought. We will present more detailed simulations in forthcoming papers.

### 3.2 The initial conditions

The parameters of the Pop-III stars are taken from Heger & Woosley (2002). We concentrate on the model having a He core mass of  $130 M_{\odot}$ , corresponding to an initial mass of about  $260 M_{\odot}$ . The explosion energy of this model Pop-III star is about  $10^{53}$  erg. This model Pop-III star releases  $40 M_{\odot}$  of Fe. If mixed with  $10^7 M_{\odot}$  of pristine gas, this amount of iron leads to a  $[\text{Fe}/\text{H}]$  of about -2.5, which is the minimum  $[\text{Fe}/\text{H}]$  observed in GCs. Lacking a detailed description of mixing processes, we will assume henceforth that the Pop-III explosion leads instantaneously to a uniform metallicity of  $[\text{Fe}/\text{H}]=-2.5$  in the supershell, which is thus also the metallicity of our 1G stars. As we will see below, the mass of gas accumulated in the supershell is generally less than  $10^7 M_{\odot}$ , thus the supershell metallicity might be higher than -2.5. Our choice is thus conservative: cooling and star formation might be more efficient than we assume in what follows.

Several papers in the literature have been devoted to the study of the formation and explosion of very massive Pop-III stars (see e.g. Abel et al. 2002; Ripamonti et al. 2002; Omukai & Palla 2003; Bromm et al. 2009; Hummel et al. 2016). We choose here to fix the initial conditions of the ISM surrounding the Pop-III star sitting in the middle of an ISM cloud according to the results of Yoshida et al. (2006).

In their study, the ISM clouds are characterized by a very small core, a very high central density and a  $r^{-2}$  envelope beyond the core. Namely the number density is characterized by the following profile:

$$n(r) = \begin{cases} n_c & \text{if } r < r_c \\ n_c \left(\frac{r}{r_c}\right)^{-2} & \text{if } r \geq r_c \end{cases} \quad (1)$$

Typical values found in the simulations of Yoshida et al. (2006) are  $r_c = 1$  au for the core radius and  $n_c = 2 \cdot 10^{15} \text{ cm}^{-3}$  for the central number density. This central density is very high, but it falls off very rapidly. The total mass contained in the whole computational grid (a sphere of radius 200 pc) is  $\sim 3 \cdot 10^6 M_{\odot}$ . Therefore, by adopting these initial conditions we are unable with the mass available to reproduce the most massive GCs observed in the Galaxy, i.e. those with masses of the order of  $10^6 M_{\odot}$ . We consider a minimum temperature of the ISM of 50 K. If dictated by the cosmic microwave background alone, this temperature implies a redshift of formation of the Pop-III star of about 17.

### 3.3 The numerical code

We construct a 1-D, Eulerian, spherically symmetric code to follow the expansion and fragmentation of the supershell produced by the Pop-III explosion. Of course, it is highly unlikely that the system will maintain a perfect spherical symmetry during the whole evolution. As mentioned before, we plan here to perform a simplified feasibility study; more detailed 3-D simulations are planned and will be presented in forthcoming papers. The code, which is second-order accurate, is based on a HLLC Riemann solver and uses slope limiters to avoid spurious oscillations (Toro 2009). The cells are uniform and 0.01 pc wide. This means that the core of 1 au in the initial ISM distribution is not resolved in our simulation. As already mentioned, we avoid the (uncertain) simulation of the process of chemical enrichment of the supershell due to the Pop-III ejecta and consider from the beginning a constant metallicity of  $[\text{Fe}/\text{H}]=-2.5$ . The physical processes included in our simulations are:

- Molecular and atomic cooling. For  $T > 10^{3.8}$  K we adopt the cooling function and the ionization fractions of Schure et al. (2009) with fitting formulae taken from Vorobyov et al. (2015). Below  $10^{3.8}$  K we adopt the atomic and molecular cooling of Dalgarno & McCray (1972). The ionization fractions are adapted from Abel et al. (1997).

- Self-gravity. The gravitational acceleration is calculated as  $g = -GM(r)/r^2$ , where  $G$  is the gravitational constant and  $M(r)$  is the mass in gas and stars contained within radius  $r$ .
- Thermal conduction. A Spitzer-type thermal conduction equation is solved by means of the Crank-Nicolson method. We refer to Bedogni & Dercole (1986) for the numerical implementation of this method.

We follow the expansion of a supershell created by the Pop-III star until it fragments and forms 1G stars. Later, we follow the evolution of the system when SSSs start inject energy and chemical elements into the ISM. Thus we include in the simulations two additional physical processes:

- Feedback from a single stellar population. This is calculated by means of a tailored Starburst99 simulation (Leitherer et al. 1999, 2014). The IMF of the SSS is assumed to be the Kroupa IMF, as it closely resembles the spectrum of mass fragments in an unstable supershell (Tenorio-Tagle et al. 2003). The energy produced by SSSs is inserted as thermal energy. Energy, gas mass, and mass in chemical elements produced by the SSSs are inserted in those grid cells, where stars reside (see below for the dynamics of the stars). The amount of feedback to be inserted in each cell is proportional to the total stellar mass in any given cell.
- Dynamics of stars. Here, we will simply assume that the stars inherit the velocity of the supershell at the moment of fragmentation. Subsequently, their dynamics is dictated by the competition between their inertia and the gravitational pull. The stellar population formed in the supershell is subdivided into 250 mass bins, each of which evolves independently. To guarantee a spread in the stellar bins, we distribute the velocities according to a Maxwellian distribution, centered on the supershell expansion velocity. Of course, our treatment grossly simplifies the dynamics of the stars, and only detailed N-body simulations can shed light on the final fate of SSSs.

Many other physical phenomena which might be relevant for the problem at hand have not been considered. As already mentioned, this has been done on purpose, in order to simplify the treatment and put more emphasis on the feasibility of the proposed scenario. A critical assessment of the missing physics will be presented in Sect. 5.

### 3.4 The fragmentation of the supershell

The ambient ISM is unlikely to be perfectly isotropic, and when accreted, it seeds the supershell with per-

turbations in its surface density. We assume that the amplitudes of perturbations are small leaving the spherically symmetric model of the expanding supershell still justified. Since our one dimensional model cannot follow shell fragmentation in three dimensional space, we estimate the time  $t_{frag}$  of the supershell fragmentation as an instant when the shell expansion time  $t$  equals to the collapse time-scale  $t_{col}$  of the most unstable fragment in the shell. Note that the fragment collapses in the direction tangent to the shell surface. Following (Whitworth et al. 1994a), the collapse time-scale is

$$t_{col} = \left\{ \frac{G\Sigma}{d} - \frac{a_s^2}{d^2} \pm \frac{\alpha^2}{t^2} \right\}^{-1/2}, \quad (2)$$

where  $\Sigma$  is the surface density,  $d$  the fragment radius,  $a_s$  the sound speed inside of the shell, and  $\alpha$  the exponent in the shell expansion law,

$$R = Kt^\alpha. \quad (3)$$

The first term on the right hand side of eq. (2) expresses the tendency of the self-gravity to bind the fragment together while the second is due to the thermal pressure gradient acting in the opposite direction. The third term describes either stretching of the fragment in the case of the expanding shell (negative sign), or the fragment contraction in the case of the collapsing shell (positive sign). The latter case applies to the secondary inward propagating shell formed by the 1G SSSs.

In the case of a supernova explosion at the density peak of a medium with a power-law density profile following equation (1), the exponent of the expanding law in the energy conserving phase is  $\alpha = 2/3$  and in the momentum conserving phase  $\alpha = 1/2$  (Ostriker & McKee 1988). The high density in our model results in rapid cooling, so the supershell switches from the energy conserving phase to momentum conserving phase very early (see also Haid et al. (2016)), and fragmentation takes place in the momentum conserving phase with  $\alpha = 1/2$ .

The relative importance of the self-gravity and external pressure in confining the supershell significantly influences the fragmentation process and the supershell fragmentation time  $t_{frag}$  (Dinnbier et al. 2017). In Appendix A, we show that the supershell likely fragments when dominated with its self-gravity, in which case the collapse time-scale of the most unstable fragment in the supershell is

$$t_{col} = \left( \frac{G^2\Sigma^2}{4a_s^2} \pm \frac{\alpha^2}{t^2} \right)^{-1/2}. \quad (4)$$

During the simulation, we evaluate  $t_{col}$  at each time step, and identify the fragmentation time  $t_{frag}$  as the

time when the expansion time  $t$  exceeds the collapse time-scale  $t_{col}$  for the first time. We assume that the SSSs are formed at this instant. The surface density,  $\Sigma$ , and the sound speed,  $a_s$ , in the shell are measured in the simulation by averaging between the inner and the outer edges of the shell, detected as the steepest positive and negative density gradients. Note that the sound speed is almost always constant with a value corresponding to the temperature 50 K as the shell is nearly isothermal (see Figure 4).

## 4 Results

Here we present results of 1D simulations modelling the supershells formed after an explosion of a Pop-III star releasing energy  $10^{53}$  ergs into a centre of a gaseous cloud with the density profile given by eq. (1). The primary expanding supershell leading to the formation of 1G stars is described in Sect. 4.1. The secondary, inward propagating supershell out of which the LG stars form is described in Sect. 4.2. Two versions of the model are studied differing in the location within the primary supershell where the 1G SSSs are inserted.

### 4.1 The expanding supershell and the formation of 1G stars

The evolution of the ISM density following the Pop-III explosion is shown in Fig. 2. As mentioned in Sect. 3.4, we expect the external shock to expand approximately as  $t^{1/2}$ . A reverse shock starts to appear in the last time-frames of this plot. Figure 3 shows the velocity, which decreases with time as expected. Figure 4 shows the sound speed  $a_s$  for the same time frames as in the previous plots. Apart from a very narrow spike, the sound speed within the supershell is constant, because the efficient cooling leads rapidly to the temperature equal to the minimum temperature of 50 K in the shocked supershell gas. The constancy of the sound speed justifies the considerations and the analytical estimates made in the previous section. Fig. 5 shows the pressure profile for the same time frames.

In this model, the fragmentation of the supershell occurs, according to the condition eq. (4), at  $t_{frag} \simeq 4.8$  Myr, an instant in which the external shock has reached the radius  $\sim 20$  pc. This corresponds to the dotted-short dashed line in Figs. 2 and 3. At this instant, the supershell has a mass of slightly more than  $3 \cdot 10^5 M_\odot$ . Assuming a star formation efficiency of 30%, we obtain a mass in SSSs of  $\sim 10^5 M_\odot$ . Since we expect the large majority of these SSSs to become unbound (see the discussion in Sect. 3.1), even considering LG

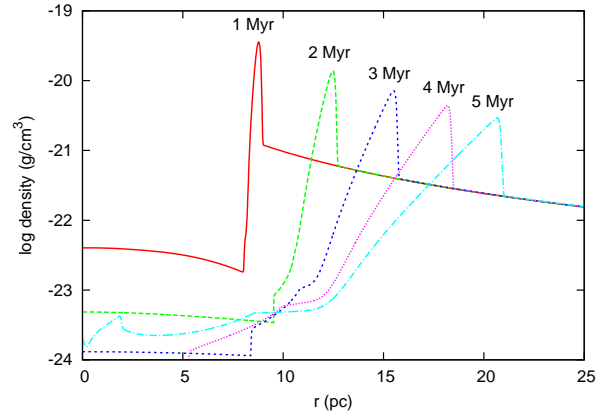


**Fig. 2** Evolution of the gas density (in  $\text{g cm}^{-3}$ ) after a Pop-III explosion. The density is plotted every Myr.

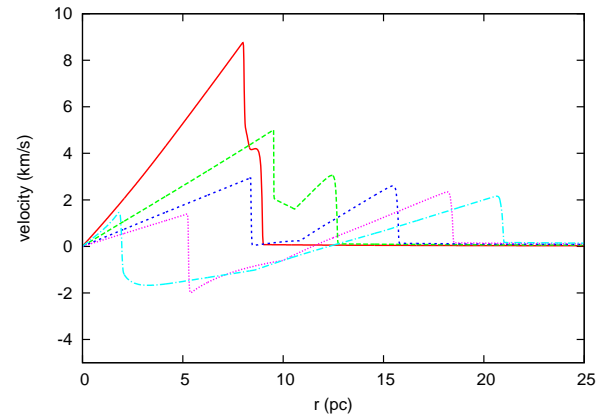


**Fig. 3** Gas velocity (in  $\text{km/s}$ ) after a Pop-III explosion, plotted every Myr as in Fig. 2.

stars we will not be able to form a GC larger than a few times  $10^4 M_\odot$ . This is consistent with the low-mass end of the mass distribution function of observed GCs; it seems much harder to obtain masses of the order of  $\sim 10^6 M_\odot$ , corresponding to the most massive observed GCs.

We have also tried to run models with densities larger than the ones described in Sect. 3.2, namely with a central density of  $n_c = 6 \cdot 10^{15} \text{ cm}^{-3}$ . In this case, the fragmentation of the supershell occurs earlier, at  $t_{frag} \simeq 0.6$  Myr (eq. (4)). However, given the higher density, the mass accumulated in the supershell at this moment in time is more or less the same. With some fine-tuning, we are able to increase the mass of the supershell by a factor of a few, but with our assumptions and initial conditions it seems impossible to accumulate substantially more mass in the supershell. It seems thus that the problem of having a supershell massive enough has more to do with the profile rather than to the central density. We have tried different, flatter initial ISM density distributions and we can pro-



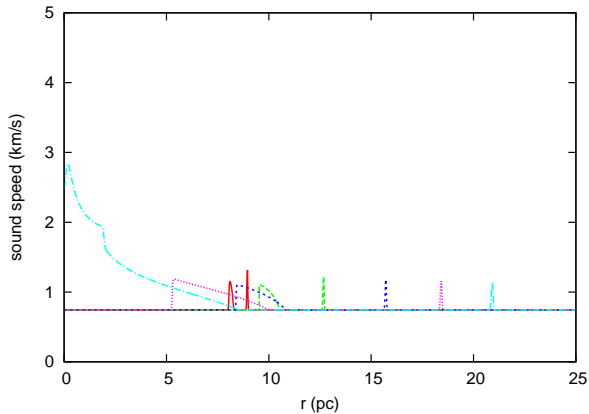


**Fig. 4** Sound speed (in km/s) after a Pop-III explosion, plotted every Myr as in Fig. 2.

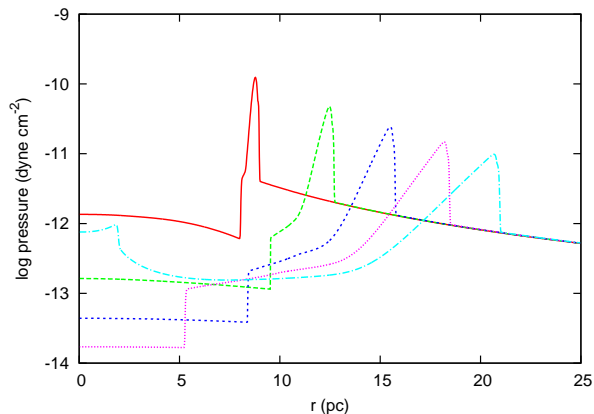


**Fig. 5** Logarithm of the pressure (in cgs) after a Pop-III explosion, plotted every Myr as in Fig. 2.

duce in this way unstable supershells with masses up to  $\sim 10^7 M_{\odot}$ . Notice that the  $r^{-2}$  profile found by Yoshida et al. (2006) extends only up to a few pc, thus a different and perhaps flatter gas distribution outside the first few pc is conceivable. We prefer in this work to stick to the Yoshida et al. (2006) initial conditions in order to study the basic scenario in a simple and well-justified setting. We will change the initial conditions in forthcoming papers. In the meantime we note that a flatter initial gas distribution would not only allow a larger total GC mass, but might also help to capture more SN ejecta, because it would be harder for them to escape outwards. That would explain why only most massive GCs exhibit variation in Fe content (and other heavy elements), as described in Sect. 2.

#### 4.2 The inward-propagating supershell and the formation of LG stars

Once the supershell has fragmented and formed new stars (the SSSs), we wish to follow the evolution of

the SSS ejecta and analyze under what conditions can these ejecta, perhaps mixing with some pristine gas, lead to the formation of new stars. The first problem we face is to figure out what is the exact location of these SSSs. As we can see from Fig. 2, the supershell is initially pretty narrow, but it broadens as time goes on. This broadening is partially deceptive given the logarithmic scale: the large majority of the supershell mass is confined within 0.5 pc behind the shock, even in the last plotted moment in time. Still, lacking a detailed physical description of the star formation process, there is still considerable uncertainty about the birth site of SSSs. One might argue that stars, being collisionless, are not slowed down by the pressure of the external medium and so might overtake the supershell. This argument is however weakened by the fact that stars form out of the densest, coolest clumps of ISM in the supershell. Pressure gradients between the center and the supershell are steeper along directions that do not cross these dense clumps and, as is well known, large pressure gradients favour a faster expansion of the supershell. Moreover, supershell expansion in non-uniform media may lead to the development of Rayleigh-Taylor instabilities. The clumps of denser gas formed as a consequence of the Rayleigh-Taylor instabilities are more severely decelerated and tend to lag behind the expanding shock (see e.g. Mueller et al. 1991; Dohm-Palmer & Jones 1996). For this reason, we decide to initially place the SSSs close to the base of the supershell, at a distance of  $\sim 16$  pc from the center. We label this *Model 1*. This choice has the further advantage that the spherical volume of radius 16 pc has been almost completely evacuated of pristine gas. Only about  $8 \times 10^3 M_{\odot}$  of gas are contained in this volume. Therefore, the ejecta of the SSSs propagating inwards are mixed with just a small fraction of pre-existing gas. As a comparison, we consider also another *Model 2* in which the SSSs are placed close to the density peak of the supershell, at a distance of 20.6 pc from the center.

As already mentioned, the feedback from the SSSs is calculated by means of tailored Starburst99 simulations. The evolution of density after the formation of SSSs for Model1 is shown in Fig. 6. It is clear that the stellar winds propagate in part towards the center, piling up the little gas remaining in the cavity. On the other hand, the original supershell continues its propagation outwards. A two-shell structure is formed. The inner supershell cools relatively quickly and becomes denser. The fragmentation time, calculated again as described in Sect. 3.4, becomes equal to the evolutionary time at  $t \simeq 0.6$  Myr after the insertion of the SSSs, which also the last moment in time plotted in Fig. 6. Notice that, in order to calculate the fragmentation time, we use the positive sign of the term  $\alpha^2/t^2$

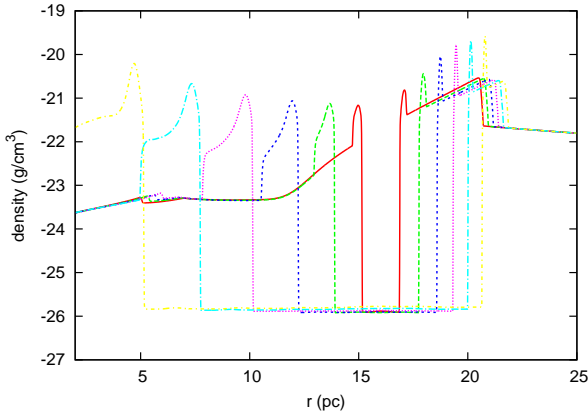


**Fig. 6** Evolution of the gas density (in  $\text{g cm}^{-3}$ ) after the formation of SSSs for Model 1. The density is plotted every 0.1 Myr after  $t = t_{frg}$  starting with the solid red line.

in Eq. 4. However, this term turns out to be much smaller than the  $G^2\Sigma^2/4a_s^2$  term. At this moment, the inner supershell has reached a distance of  $\sim 5$  pc from the center, and has accumulated slightly more than  $10^4 M_\odot$  of gas. A significant, but still relatively low (about 20 %) fraction of this gas is made of ejecta of SSSs, which were able to cool in a short timescale. This short cooling timescale is due to the large densities of the supershell. The fact that the fraction of SSS ejecta in the inward-propagating supershell is relatively low is due to the fact that, with our adopted Starburst99 model, the amount of material ejected by stellar winds in the first Myr is quite low. It increases and becomes significant only after 3-4 Myr.

*Model 2* takes a longer time to propagate towards the center and to fragment, mainly due to the higher densities the supershell has to travel through. The fragmentation occurs after  $\sim 3$  Myr, when the inward-propagating supershell has reached a distance of  $\sim 8$  pc from the center (see Fig. 7). The mass of the unstable supershell at this point is relatively large (about  $10^5 M_\odot$ ), but the majority of this gas is pristine, thus the ejecta of the SSSs can not pollute significantly the new generation of stars. The energy of the SSSs is simply pushing the pre-existing supershell inwards. Notice that at an age of 3 Myr the first SNe start exploding. Although we do not see the signs of contamination of SN ejecta in this specific model, it is at least conceivable that some GCs might form LG stars partially polluted by ejecta of Type II SNe.

## 5 Discussion and conclusions

In this work we have studied the explosion of a very energetic Pop-III star and the subsequent supershell ex-

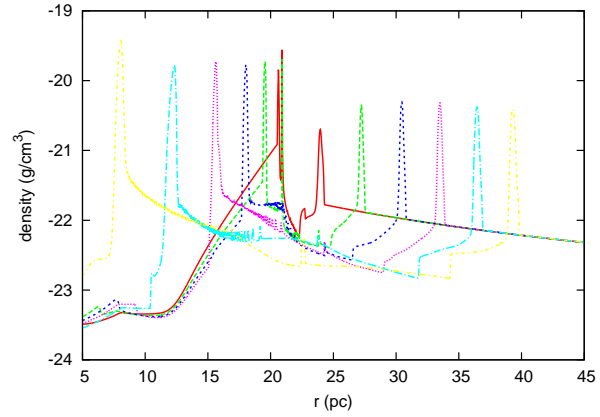


**Fig. 7** Evolution of the gas density (in  $\text{g cm}^{-3}$ ) after the formation of SSSs for Model 2. The density is plotted every 0.5 Myr after  $t = t_{frg}$  starting with the solid red line.

pansion. This supershell becomes gravitationally unstable and fragments and, eventually, starts forming stars. Depending on the explosion energy and on the central density of the ISM surrounding the Pop-III star, gravitational instabilities start growing  $\sim 0.5$ –5 Myr after the Pop-III explosion, and eventually lead to the formation of supershell stars (SSSs). The fate of the ejecta of these SSSs is the main aim of this paper. We have seen that the energy of SSS stellar winds is able in part to accelerate the already existing supershell created by the Pop-III, in part to create a new, inward-propagating supershell. With our assumptions, this supershell is particularly rich in SSS ejecta, at least if we assume that the SSSs are initially located close to the inner edge of the supershell. This supershell is able to cool in a very short time (a fraction of a Myr), due to its very large density. We have also checked that this inward-propagating supershell also becomes gravitationally unstable and might lead to a new generation of stars. There is thus the possibility to repeat the already described process and create a new inward-propagating supershell and, from it, a new stellar population. For the moment we have limited our analysis to the study of the formation of this second generation of stars, but we intend to analyze the possibility to form a third generation of stars in a future work.

We have considered also if our depicted scenario can help explaining some of the puzzling aspects of globular clusters (GCs). In particular, we wanted to see whether it can explain some characteristics of GC stars listed in Sect. 2, namely specificity, predominance, discreteness and supernova avoidance.

Our scenario certainly helps explaining the specificity of GCs, as it singles out one physical process which was present only in the early Universe (Pop-III stars); see also the discussion in Sect. 3.1. It can help

also explain the predominance of late generation (LG) stars as compared to the first generation. We have seen that, depending on the explosion energy and on the central density, the supershell can fragment and form new stars at a distance between 4 and 20 pc from the center of the explosion. LG stars form much closer to the cluster center, so they have a higher chance to remain bound to the cluster than first generation (1G) stars (our SSSs). Moreover, SSSs are born with a positive radial velocity, at variance with LG stars, and this increases the chance that a large fraction of 1G stars might be unbound. Even if this argument is sound, our simulations can not make quantitative predictions on that and we have to wait for N-body simulations to shed light on the different dynamics and on the fate of 1G and LG stars. As explained in Sect. 2, Milone et al. (2017) find a clear correlation between the mass of a GC and the fraction of 1G stars. This fraction is large for low-mass clusters and decreases with increasing GC mass. Also this result is broadly consistent with our scenario. In fact, we expect that, if the supershell formed by the Pop-III star is large, then a large number of 1G stars can be formed. These stars however, due to the large distance of the supershell, have a larger probability of escaping the gravitational potential. As we have seen (Sect. 3.1), the dependence of the chemical complexity in GCs on the stellar mass might also be accounted for in our model. However, it was not our intention in this paper to provide a detailed model of the chemical composition of GCs. The abundances of different elements are taken from a Starburst99 model, and this is probably inadequate to account for the chemical peculiarities of GCs. The time evolution of the content of He, C, N, O, Na, Si and of other elements will be the subject of a subsequent paper. Also as regards the dynamics of stars, although the argument presented here is sound, still we have to wait for N-body simulations for a detailed quantitative analysis.

We conclude this paper with a quick discussion on the comparison between GCs in the Milky Way and in the Magellanic Clouds. Most GCs in the LMC and SMC with ages smaller than  $\sim 2$  Gyr show an extended main-sequence turn off (Mackey et al. 2008; Milone et al. 2009, 2016). Although the connection between this spread and the presence of multiple stellar populations is still not firmly established, the impression is that young and intermediate-age clusters in Magellanic clouds are the counterparts of old GCs with multiple populations (Conroy & Spergel 2011). This connection is fascinating although only measurements of abundances of individual stars (for which we must wait JWST) can tell us whether we might face for GCs in

the Magellanic Clouds the same problems we face for Milky Way GCs. For the moment we note that the model of a collapsing supershell may also apply to intermediate age clusters in the LMC and SMC if there was a sufficiently strong source of energy. This source of energy might also be due to a Pop-III star, but this is unlikely to be the case for young GCs.

### Acknowledgements

Support for this project was provided by the Czech Science Foundation grant 15-06012S and by the project RVO: 6785815. We thank the anonymous referee for very useful and insightful remarks and suggestions. We thank Sona Ehlerova and Anthony Whitworth for assistance with the preparation of the manuscript.

## References

- Abel, T., Anninos, P., Zhang, Y., & Norman, M. L. 1997, *New Astron.*, 2, 181
- Abel, T., Bryan, G. L., & Norman, M. L. 2002, *Science*, 295, 93
- Bastian, N. 2015, arXiv:1510.01330
- Bastian, N., Cabrera-Ziri, I., Davies, B., & Larsen, S. S. 2013, *Mon. Not. R. Astron. Soc.*, 436, 2852
- Bastian, N., Lamers, H. J. G. L. M., de Mink, S. E., et al. 2013, *Mon. Not. R. Astron. Soc.*, 436, 2398
- Bastian, N., & Lardo, C. 2015, *Mon. Not. R. Astron. Soc.*, 453, 357
- Beasley, M. A., Kawata, D., Pearce, F. R., Forbes, D. A., & Gibson, B. K. 2003, *Astrophys. J. Lett.*, 596, L187
- Bedogni, R., & Dercole, A. 1986, *Astron. Astrophys.*, 157, 101
- Bisnovatyi-Kogan, G. S., & Silich, S. A. 1995, *Reviews of Modern Physics*, 67, 661
- Bromm, V., Coppi, P. S., & Larson, R. B. 1999, *Astrophys. J. Lett.*, 527, L5
- Bromm, V., Yoshida, N., Hernquist, L., & McKee, C. F. 2009, *Nature*, 459, 49
- Brown, J. H., Burkert, A., & Truran, J. W. 1991, *Astrophys. J.*, 376, 115
- Cabrera-Ziri, I., Lardo, C., Davies, B., et al. 2016, *Mon. Not. R. Astron. Soc.*, 460, 1869
- Carretta, E. 2015, *Astrophys. J.*, 810, 148
- Charbonnel, C., & Chantereau, W. 2016, *Astron. Astrophys.*, 586, A21
- Choplin, A., Meynet, G., Maeder, A., Hirschi, R., & Chiappini, C. 2016, arXiv:1602.04122
- Conroy, C., & Spergel, D. N. 2011, *Astrophys. J.*, 726, 36
- Dalgarno, A., & McCray, R. A. 1972, *Annu. Rev. Astron. Astrophys.*, 10, 375
- Denissenkov, P. A., Vandenberg, D. A., Hartwick, F. D. A., et al. 2015, *Mon. Not. R. Astron. Soc.*, 448, 3314
- de Mink, S. E., Pols, O. R., Langer, N., & Izzard, R. G. 2009, *Astron. Astrophys.*, 507, L1
- D’Ercole, A., D’Antona, F., Ventura, P., Vesperini, E., & McMillan, S. L. W. 2010, *Mon. Not. R. Astron. Soc.*, 407, 854
- D’Ercole, A., Vesperini, E., D’Antona, F., McMillan, S. L. W., & Recchi, S. 2008, *Mon. Not. R. Astron. Soc.*, 391, 825
- Decressin, T., Charbonnel, C., Meynet, G. 2007, *Astron. Astrophys.*, 475, 859
- Dinnbier, F., Wünsch, R., Whitworth, A. P., & Palouš, J. 2017, *Mon. Not. R. Astron. Soc.*, 466, 4423
- Dohm-Palmer, R. C., & Jones, T. W. 1996, *Astrophys. J.*, 471, 279
- Ehlerova, S., Palous, J., Theis, C., & Hensler, G. 1997, *Astron. Astrophys.*, 328, 121
- Elmegreen, B. G. 1994, *Astrophys. J.*, 427, 384
- Elmegreen, B. G. 2017, *Astrophys. J.*, 836, 80
- Elmegreen, B. G., & Elmegreen, D. M. 1978, *Astrophys. J.*, 220, 1051
- Gerola, H., & Seiden, P. E. 1978, *Astrophys. J.*, 223, 129
- Gratton, R., Sneden, C., & Carretta, E. 2004, *Annu. Rev. Astron. Astrophys.*, 42, 385
- Haid, S., Walch, S., Naab, T., et al. 2016, *Mon. Not. R. Astron. Soc.*, 460, 2962
- Harris, W. E. 1996, *Astron. J.*, 112, 1487
- Heger, A., & Woosley, S. E. 2002, *Astrophys. J.*, 567, 532
- Heger, A., & Woosley, S. E. 2010, *Astrophys. J.*, 724, 341
- Hummel, J. A., Stacy, A., & Bromm, V. 2016, *Mon. Not. R. Astron. Soc.*, 460, 2432
- Johnson, C. I., Caldwell, N., Rich, R. M., et al. 2017, *Astrophys. J.*, 842, 24
- Krause, M., Charbonnel, C., Decressin, T., Meynet, G., & Prantzos, N. 2013, *Astron. Astrophys.*, 552, A121
- Leitherer, C., Ekström, S., Meynet, G., et al. 2014, *Astrophys. J. Suppl. Ser.*, 212, 14
- Leitherer, C., Schaerer, D., Goldader, J. D., et al. 1999, *Astrophys. J. Suppl. Ser.*, 123, 3
- Lochhaas, C., & Thompson, T. A. 2017, *Mon. Not. R. Astron. Soc.*, 470, 977
- Mackey, A. D., Broby Nielsen, P., Ferguson, A. M. N., & Richardson, J. C. 2008, *Astrophys. J. Lett.*, 681, L17
- Marino, A. F., Milone, A. P., Karakas, A. I., et al. 2015, *Mon. Not. R. Astron. Soc.*, 450, 815
- Marino, A. F., Sneden, C., Kraft, R. P., et al. 2011, *Astron. Astrophys.*, 532, A8
- Marino, A. F., Villanova, S., Piotto, G., et al. 2008, *Astron. Astrophys.*, 490, 625
- Milone, A. P. 2015, *Mon. Not. R. Astron. Soc.*, 446, 1672
- Milone, A. P., Bedin, L. R., Piotto, G., & Anderson, J. 2009, *Astron. Astrophys.*, 497, 755
- Milone, A. P., Marino, A. F., D’Antona, F., et al. 2016, *Mon. Not. R. Astron. Soc.*, 458, 4368
- Milone, A. P., Marino, A. F., Piotto, G., et al. 2015, *Mon. Not. R. Astron. Soc.*, 447, 927
- Milone, A. P., Marino, A. F., Piotto, G., et al. 2015, *Astrophys. J.*, 808, 51
- Milone, A. P., Piotto, G., Renzini, A., et al. 2017, *Mon. Not. R. Astron. Soc.*, 464, 3636
- Mueller, E., Fryxell, B., & Arnett, D. 1991, *Astron. Astrophys.*, 251, 505
- F. Niederhofer, N. Bastian, V. Kozhurina-Platais, S. Larsen, K. Hollyhead, C. Lardo, I. Cabrera-Ziri, N. Kacharov, I. Platais, M. Salaris, M. Cordero, E. Dalessandro, D. Geisler, M. Hilker, C. Li, D. Mackey, A. Mucciarelli 2017, *Mon. Not. R. Astron. Soc.*, 465, 4159
- Omukai, K., & Palla, F. 2003, *Astrophys. J.*, 589, 677
- Ostriker, J. P., & McKee, C. F. 1988, *Reviews of Modern Physics*, 60, 1
- Palous, J., Tenorio-Tagle, G., & Franco, J. 1994, *Mon. Not. R. Astron. Soc.*, 270,
- Pancino, E., Romano, D., Tang, B., et al. 2017, *Astron. Astrophys.*, 601, A112
- Parmentier, G., Jehin, E., Magain, P., et al. 1999, *Astron. Astrophys.*, 352, 138
- Piotto, G., Bedin, L. R., Anderson, J., et al. 2007, *Astrophys. J. Lett.*, 661, L53
- Placco, V. M., Frebel, A., Beers, T. C., et al. 2016, *Astrophys. J.*, 833, 21
- Recchi, S., & Danziger, I. J. 2005, *Astron. Astrophys.*, 436, 145
- Renzini, A., D’Antona, F., Cassisi, S., et al. 2015, *Mon. Not. R. Astron. Soc.*, 454, 4197



- 
- Ripamonti, E., Haardt, F., Ferrara, A., & Colpi, M. 2002, *Mon. Not. R. Astron. Soc.*, 334, 401
- Schure, K. M., Kosenko, D., Kaastra, J. S., Keppens, R., & Vink, J. 2009, *Astron. Astrophys.*, 508, 751
- Shustov, B. M., & Wiebe, D. S. 2000, *Mon. Not. R. Astron. Soc.*, 319, 1047
- Snedden, C., Kraft, R. P., Shetrone, M. D., et al. 1997, *Astron. J.*, 114, 1964
- Tenorio-Tagle, G., Palouš, J., Silich, S., Medina-Tanco, G. A., & Muñoz-Tuñón, C. 2003, *Astron. Astrophys.*, 411, 397
- Toro, E.F. 2009, *Riemann Solvers and Numerical Methods for Fluid Dynamics: A Practical Introduction*. Third Edition. Springer-Verlag Berlin Heidelberg.
- Vishniac, E. T. 1983, *Astrophys. J.*, 274, 152
- Vorobyov, E. I., Recchi, S., & Hensler, G. 2015, *Astron. Astrophys.*, 579, A9
- Whitworth, A. P., Bhattal, A. S., Chapman, S. J., Disney, M. J., & Turner, J. A. 1994, *Mon. Not. R. Astron. Soc.*, 268, 291
- Whitworth, A. P., Bhattal, A. S., Chapman, S. J., Disney, M. J., & Turner, J. A. 1994, *Astron. Astrophys.*, 290, 421
- Wünsch, R., & Palouš, J. 2001, *Astron. Astrophys.*, 374, 746
- Wünsch, R., Palouš, J., Tenorio-Tagle, G., Muñoz-Tuñón, C., & Ehlerová, S. 2016, [arXiv:1601.03867](https://arxiv.org/abs/1601.03867)
- Wünsch, R., Palouš, J., Tenorio-Tagle, G., & Ehlerová, S. 2017, *Astrophys. J.*, 835, 60
- Yong, D., Da Costa, G. S., & Norris, J. E. 2016, *Mon. Not. R. Astron. Soc.*, 460, 1846
- Yong, D., Roederer, I. U., Grundahl, F., et al. 2014, *Mon. Not. R. Astron. Soc.*, 441, 3396
- Yoshida, N., Omukai, K., Hernquist, L., & Abel, T. 2006, *Astrophys. J.*, 652, 6

## A The role of the external pressure on supershell fragmentation

Dinnbier et al. (2017) suggest that the relative importance of the pressure  $P_{ext}$  confining a shell influences the fragmentation not only quantitatively, but also qualitatively. If the confining pressure dominates the self-gravity, the shell breaks into many gravitationally stable objects which subsequently coalesce until they form enough mass to collapse gravitationally. If the self-gravity dominates the confining pressure, the condensing fragments collapse directly into gravitationally bound objects. While the dispersion relation proposed by Elmegreen & Elmegreen (1978) provides a reasonable estimate for fragment properties for self-gravity dominated shells, no linearised estimate holds for pressure dominated shells. For pressure dominated shells, Dinnbier et al. (2017) indicate that the Jeans mass is a proxy for the fragment mass. This determines our choice of fragment radius  $d$  and the approximations made in eq. (2) in these two cases. For pressure-dominated shells, we assume that the most unstable fragment contains one Jeans mass while for self-gravity dominated shells, we assume that the radius corresponds to the most unstable wavelength in the dispersion relation proposed by Elmegreen & Elmegreen (1978). Therefore,

$$d = \begin{cases} \frac{\sqrt{1.5A}a_s^2}{G\Sigma} & \text{pressure dominated shell} \\ \frac{2a_s^2}{G\Sigma} & \text{self-gravity dominated shell} \end{cases} \quad (\text{A1a})$$

where parameter

$$A = \frac{1}{\sqrt{1 + 2P_{ext}/(\pi G\Sigma^2)}} \quad (\text{A2})$$

indicates the relative importance of the external pressure versus self-gravity (Elmegreen & Elmegreen 1978). Parameter  $A$  lies in the interval  $(0, 1)$ , where pressure dominated shells have  $A$  near zero and self-gravity dominated ones  $A$  near unity.

Since fragmentation occurs at substantially different times for pressure dominated and self-gravity dominated shells, we investigate which case is more appropriate to our supershell model and use the approximation for the fragmenting time accordingly. Let us assume that the supershell fragments in the pressure dominated case. For this reason, we omit the second term on the right hand side of eq. (2) because unstable fragments are delivered by coalescence with no role of the pressure gradient. The sound speed of the supershell  $a_s$  is insensitive to the position within the supershell wall (see Figure 4). The sound speed also changes very little during the expansion. This enables us to express the fragmenting time in the closed form.

Let us assume a supernova explosion at the density peak of a medium with a general power-law density distribution  $n(r) = n_c(r/r_c)^{-\omega}$ . The exponent of the expanding law  $\alpha$  (equation 3) depends on the value of  $\omega$  and whether the shell is in the energy conserving phase or the momentum conserving phase. While for expansion in the energy conserving phase  $\alpha = 2/(5 - \omega)$ , for expansion in the momentum conserving phase  $\alpha = 1/(4 - \omega)$  (Ostriker & McKee 1988).

The surface density of a supershell of radius  $R$  is

$$\Sigma(R) = \frac{M(R)}{4\pi R^2} = \frac{n_c \bar{m} r_c^2 K^{1-\omega} t^{\alpha(1-\omega)}}{3 - \omega}, \quad (\text{A3})$$

where  $\bar{m}$  denotes the mean gas particle mass. The supershell is confined by two pressures: thermal pressure from the cavity acting on its inner surface, and ram pressure from the accreting medium acting on its outer surface. In the momentum conserving phase, the latter of the pressures is significantly higher than the former. For the adopted model of shell fragmentation, it is not a priori clear, which of these pressures characterises fragmentation better. We choose the ram pressure, which is higher, to represent  $P_{ext}$ , and we shall see that the shell fragments in self-gravity dominated case, so the choice of the particular pressure is not important. Thus,

$$P_{ext} = n(r)\bar{m}(\mathrm{d}R/\mathrm{d}t)^2 = n_c \bar{m} r_c^2 K^{2-\omega} \alpha^2 t^{2\alpha-\alpha\omega-2}. \quad (\text{A4})$$

Substituting eq. (A3), eq. (A4) and the parameter  $A$  for pressure dominated shells (small  $A$ ;  $P_{ext} \gg \pi G \Sigma^2$ ) where eq. (A2) becomes

$$A \simeq \left\{ \frac{\pi G \Sigma^2}{2 P_{ext}} \right\}^{1/2} = \sqrt{\frac{\pi G n_c \bar{m} r_c^2}{2} \frac{K^{-\omega/2} t^{-(\alpha\omega+2)/2}}{\alpha(3-\omega)}}, \quad (\text{A5})$$

into eq. (A1a) and eq. (2), one obtains the fragmenting time ( $t_{frag} = t_{col}$ ),

$$t_{frag} = \left\{ \frac{9\pi a_s^4 (3-\omega)^6 (1+\alpha^2)^4 K^{7\omega}}{8\alpha^2 (G n_c \bar{m} r_c^2)^7 K^8} \right\}^{1/(6+8\alpha-7\alpha\omega)}. \quad (\text{A6})$$

We use  $\alpha = 1/2$  and  $\omega = 2$  for the presented model. Substituting these values to eq. (A6) and using eq. (A2) with  $t = t_{frag}$ , we realise that the supershell fragmented when  $A \simeq 0.8$ , i.e. in the self-gravity dominated case. This finding contradicts the original assumption that the supershell fragments in the pressure dominated case.

Therefore, to estimate the fragmenting time, we use the estimate of fragment radius in the self-gravity dominated case and also take into account the term in eq. (2) representing the pressure gradient. Substituting eq. (A1b) into eq. (2), one finds that the fragment collapse time-scale is given by

$$t_{col} = \left( \frac{G^2 \Sigma^2}{4a_s^2} - \frac{\alpha^2}{t^2} \right)^{-1/2}. \quad (\text{A7})$$

Note that for shells expanding in the momentum conserving phase, the second term on the right hand side of eq. (A7) decreases faster than the first term if  $\omega < 5/2$ . Thus, for the choice  $\omega = 2$ , there always exists an expansion time  $t$  which is larger than the fragment collapse time  $t_{col}$ , and the shell fragments.